Numerical investigation of solidification and CET of the transparent alloy NPG-37.5 wt.% DC in microgravity “TRACE” experiment

2016 IOP Conf. Ser.: Mater. Sci. Eng. 117 012011

(http://iopscience.iop.org/1757-899X/117/1/012011)

IOP Conf. Series: Materials Science and Engineering **117** (2016) 012011 doi:10.1088/1757-899X/117/1/012011

Numerical investigation of solidification and CET of the transparent alloy NPG-37.5 wt.% DC in microgravity "TRACE" experiment

M Ahmadein[1,2,a], M Wu[1,3,b], L Sturz[4,c] G Zimmermann[4,d] and A Ludwig[1]
[1] Chair for Modeling and Simulation of Metallurgical Processes, University of Leoben, Austria
[2] Department of Production Engineering and Mechanical, Tanta University, Egypt
[3] Christian-Doppler Laboratory for Advanced Process Simulation of Solidification & Melting, University of Leoben, Austria
[4] ACCESS e.V., Aachen, Germany

Email: [a] mahmoud.ahmadein@unileoben.ac.at, [b] menghuai.wu@unileoben.ac.at,
[c] L.Sturz@access.rwth-aachen.de, [d] G.Zimmermann@access.rwth-aachen.de

Abstract. A solidification experiment "TRACE" of the transparent alloy Neopentylglycol (NPG)-37.5wt.% D-Camphor (DC) was conducted on-board the sounding rocket TEXUS-47 in low-gravity environment to investigate the columnar growth and the columnar-to-equiaxed transition (CET). To improve the fundamental understanding of solidification and CET in microgravity, the current laboratory scale experiment was tried to be numerically reproduced by a recently developed 5-phase volume averaging model. The temperature gradient in the solidification cell is applied to the simulation. In absence of melt flow, the calculated cooling curves, columnar tip position, tip undercooling and velocity, and number density of equiaxed crystals were compared to the results of in-situ real-time observations of the experiment. The CET could be predicted at position close to that of experiment. Simulation reveals the competitive growth between the columnar and equiaxed crystals before CET. Modelling parameters of equiaxed nucleation and columnar tip growth are the key to regulate this competition and to locate the CET. Experimental verification of modelling parameters considering melt flow is intended in the future work.

1. Introduction

Mechanical properties of alloys are directly related to their as-cast structure. Columnar growth is favoured for example in single crystal growth [1] or in some turbine blades [2]. High thermal gradient at solid/liquid interface promotes the columnar growth. Equiaxed grain structure exhibits more isotropic properties and are formed upon nucleation that can be provoked by several mechanisms: (1) heterogeneous nucleation [3]; (2) the 'big band' theory [4]; (3) partial remelting of columnar dendrites [5]; and (4) the showering down of dendrite crystals formed from the casting top surface [6]. A mixed columnar-equiaxed structure with a transition zone (CET) exhibit undesirable anisotropic mechanical properties. CET occurs if the volume faction of equiaxed grains ahead of the columnar tip front is high enough to block the advancement of the columnar tip front (hard blocking) [7]. The advancement of the columnar tip front can be decelerated or even blocked (soft blocking) if the solute concentration in the melt ahead of the front increases to the limit that the constitutional undercooling decreases or vanishes[8].

Understanding the origin of the solidification structure helps to control the structure and correspondingly the mechanical properties. Gravity has a remarkable contribution to the thermal and solutal convection of the melt and the crystal sedimentation. The transport of heat and mass are correspondingly affected. The analysis of solidification phenomenon can be simplified by reducing the aforementioned interactions in low gravity (microgravity) conditions. For this purpose a solidification experiment of the transparent alloy Neopentylglycol (NPG)-37.5wt.% D-Camphor (DC) was conducted on-board the sounding rocket TEXUS-47 in a low gravity environment [9,10]. The current work is dedicated to investigate the columnar/equiaxed competition during the micro-gravity experiment using a 5-phase mixed columnar-equiaxed solidification model [11,12]. A numerical study is conducted to adjust the model parameters for the nucleation law and the semi-empirical model of columnar tip velocity. The numerical predictions were discussed and compared to the experiment.

2. Experimental aspects

The concept of "TRACE" (TRansparent Alloy in Columnar Equiaxed solidification) is to perform directional solidification in a thin (1 mm) sample using the optically transparent model system NPG-37.5 wt.% DC alloy for in-situ and real-time observation of the solidifying dendritic microstructure, see figure 1. The thermal gradient within the container is controlled by superimposing a forced cooling at the bottom (cooler) and the top (heater) as shown in figure 2. The columnar growth is initiated by applying a cooling rate of 1/300 K/s at heater and cooler at a roughly constant gradient. An increase of the cooling rate to 1/30 K/s leads to a transition to equiaxed dendritic growth and thus to CET. Melting, mixing, homogenization of the liquid alloy and columnar growth is carried out prior to the rocket launch. The low-gravity level (below 1mg) is achieved at about 1 min after lift-off of the rocket and the high cooling rate is applied to provoke CET under diffusive conditions. Images are taken in overview and from microstructure details. The thermal profile within the alloy is measured using five type-K thermocouples with diameter 0.25 mm inserted from one side. The thermal data and video data are analysed in terms of the position, velocity and temperature of the solidification interface. The nucleation temperatures and the number density of equiaxed crystals are estimated from the experiment. In addition, the volume fractions of the columnar behind the solidification front and the equiaxed and liquid phases ahead of solidification front are determined. Further details of experimental procedure can be found elsewhere [9,10].

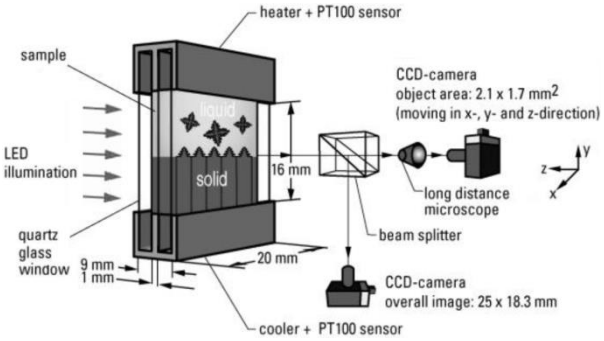

Figure 1. Schematic drawing of the main parts of the experimental setup.

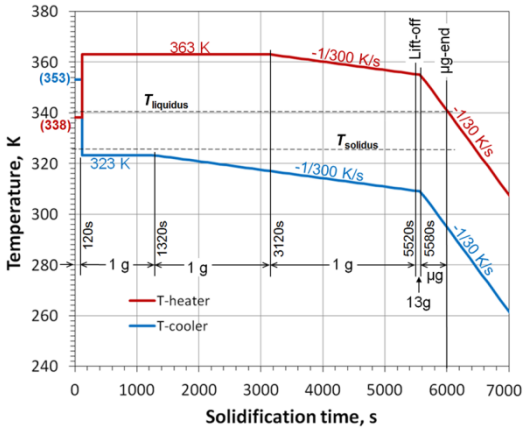

Figure 2. Cooling curves of the forced cooling system at the heater and cooler in µg experiment.

3. Model features

The 5-phase mixed columnar-equiaxed solidification model with dendritic morphology comprises three hydrodynamic phases: the liquid melt, the equiaxed crystals, and the columnar grains, denoted as l-, e- and c-phases and have corresponding volume fractions; f_l, f_e, and f_c. Globular and dendritic growth of equiaxed crystals and cellular and dendritic growth of columnar grains are considered. In

case of dendritic growth, two additional phase regions exist within each of the equiaxed and the columnar crystal envelopes: the solid dendrites with corresponding solid fractions α_s^e and α_s^c, and interdendritic melt with corresponding volume fractions α_d^e and α_d^c inside crystal envelopes. Consequently, the system encompasses five 'thermodynamic' phases: (1) the solid equiaxed dendrite and (2) the interdendritic melt within the equiaxed grain envelope, (3) the solid columnar dendrite and (4) interdendritic melt within the columnar crystal envelope, and (5) the extradendritic melt. The corresponding averaged volume fractions are: f_s^e, f_d^e, f_s^c, f_d^c, f_l referring to total volume and they are characterized by corresponding solute concentration: c_s^e, c_d^e, c_s^c, c_d^c, c_l.

The growth of the grain envelope and the solidification of the interdendritic melt are treated differently. The growth of the envelopes is determined by dendrite growth kinetics. The semi-empirical Kurz-Giovanola-Trivedi (KGT) model [12] is fitted by the polynomial given in equation (1) and is used for the growth of columnar primary dendrite tips, where $v_{tip'}^c$: growth velocity of the columnar primary dendrite tip, k_1 and k_2: model parameters. Lipton-Glicksman-Kurz (LGK) model [13] is applied for the growth of columnar secondary dendrite tips (radial growth of the columnar trunk) and equiaxed primary dendrite tips.

A heterogeneous nucleation law [15,16], equation (2), with three fitting parameters; the mean undercooling, ΔT_M, the standard deviation of undercooling, ΔT_σ, and maximum grain number density, n_{max} is used to calculate the source term for the transport equation of the equiaxed number density, n, where ΔT_{con} is the constitutional undercooling. Further details of the model are provided in [11,12].

$$v_{tip'}^c = k_1 \cdot \Delta T_{\mathrm{con}}^2 + k_2 \cdot \Delta T_{\mathrm{con}}^3 \tag{1}$$

$$\frac{dn}{d(\Delta T)} = \frac{n_{max}}{\sqrt{2\pi} \cdot \Delta T_\sigma} \cdot e^{-\frac{1}{2}\left(\frac{\Delta T_{\mathrm{con}} - \Delta T_M}{\Delta T_\sigma}\right)} \tag{2}$$

The advancement of the columnar tip front can be stopped either mechanically (hard blocking) when f_e ahead of the columnar primary tip front exceeds 0.49 [7] or thermodynamically (soft blocking) [8] when liquid melt at the columnar tip is enriched with solute to the extent that the constitutional undercooling vanishes. At this moment columnar-to-equiaxed (CET) transition occurs. The CET position is determined based on the growth competition between the c- and e-phases. The growth rate of c-phase perpendicular to cold bottom wall is calculated from equation (1) and that for e-phase is affected by the growth kinetics and the number density, n, from equation (2).

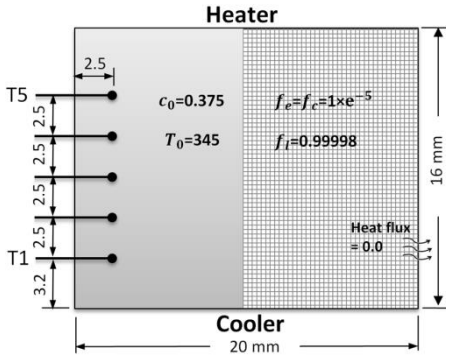

Figure 3. 2D grid of the solidification cell with boundary and initial conditions.

4. Configuration of simulation

The solidification cell of Neopentyl-glycol (NPG)-37.5wt.% D-Camphor (DC) is simplified to a 2D grid with volume element size of 0.25×0.25 mm^2 as shown in figure 3. The grid is provided by 5 measuring points (thermocouples) to record the cooling curves analogous to experiment. Similar to the experiment, a temperature gradient is applied to the simulation grid by superimposing the experiment cooling curves at the cooler and heater (Figure 2) on the corresponding grid boundaries. The conservation equations of mass, enthalpy, species, and number density are solved sequentially at each time using CFD software package, ANSYS-fluent version 14.5.0 based on the control volume method. Time step size of 0.2 s was used to achieve solution convergence over a solidification time of ~7000 s.

The thermophysical properties of NPG-37.5 wt.% DC and the modelling parameters are listed in table 1. Here ΔT_m and ΔT_σ are estimated by a Gaussian fit to experimental data and k_1 is assumed. In microgravity (µg) experiment CET occurs at ~9.5 mm above the cold boundary. This value is used to estimate the fitting n_{max} and k_2 after a numerical parameter study.

Table 1. Thermophysical properties and modelling parameters of NPG-37.5wt.% DC [9,17,18].

Thermo physical properties: c_0= 37.5 wt.% DC, c_E= 45.3 wt.% DC $T_{liquidus}$ [K]: 340.25, $T_{liquidus}$ [K]: 325.95 Liquidus slope: -1.84 K/wt.%, Partition coefficient: 0.085 Diffusion coeff. [m^2/s] liquid: 9.7×10^{-11}, solid: 8.0×10^{-20} Thermal capacity [J/kg·K] liquid: 2400, solid: 2650 Thermal conductivity [W/m·K] liquid: 0.125, solid: 0.265 Density [kg/m^3]: 1035 Latent heat of fusion [kJ/kg]: 33.4 Liquid viscosity [kg/m·s]: 6.43×10^{-3} Gibbs Thomson coefficient [Km]: 7.8e-8	**Nucleation parameters:** n_{max}= 5.0326×10^{10} m^{-3}, ΔT_σ= 4.0 K, ΔT_m = 13.5 K **Morphological parameters:** Equiaxed dendrite: Shape factor: 0.48, Sphericity: 0.4 Columnar dendrite: Shape factor: 0.7979, Trunk circularity: 0.5 λ_1= 400 µm, λ_2= 50 µm **Tip growth parameters for KGT model:** k_1= 1.1x10^{-8}, k_2 = 4.55x10^{-8}

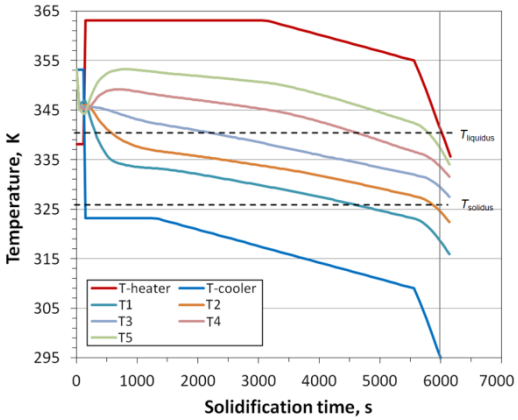

Figure 4. The calculated cooling curves in the solidification cell at positions T1-T5.

5. Results and discussion

The calculated cooling curves of the "thermocouples" 1→5 plotted in figure 4 are very similar to those from experiment [9]. The melt is supercooled at position T1 after ~300 s, whereas position T5 is supercooled at 5740 s. Increasing cooling rate after 5580 s triggers the CET. The low thermal conductivity of the alloy delays the response of the cooling curves to the cooler and heater temperatures. However, a constant temperature gradient is almost maintained.

Solidification starts at the bottom as columnar with an advancing tip front (c-front) towards the top as shown in figure 5a. Later on, equiaxed crystals nucleate and grow ahead of the c-front. The melt below the liquidus isoline is supercooled. Increasing the cooloing rate after ~5500 s expands the supercooled liquid region between c-front and liquidus isoline (figure 5b). Correspondingly, the

nucleation rate of e-phase and the growth rates of e- and -phases increase. This competition results in higher f_e ahead of the advancing c-front to surpass the blocking limit (0.49). Thus, the advancement of c-front stops and CET occurs. Thereafter (figure 5c), the solidification of e-phase continues ahead of the c-front, whereas c-phase solidify only behind the c-front. Similar to µg-experiment (figure 5d), the calculated CET occurs between T3 and T4. Nevertheless, in simulation CET occurs relatively earlier than experiment. This can be attributed to the overestimation of k_2 parameter.

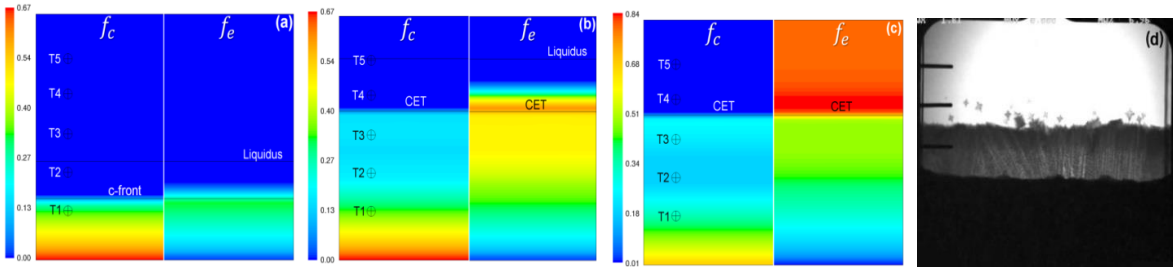

Figure 5. The calculated f_c and f_e at (a) 820 s, (b) 5820 s, and (c) 6400 s and (d) the CCD-image of the solidification cell in µg-experiment at 5955 s.

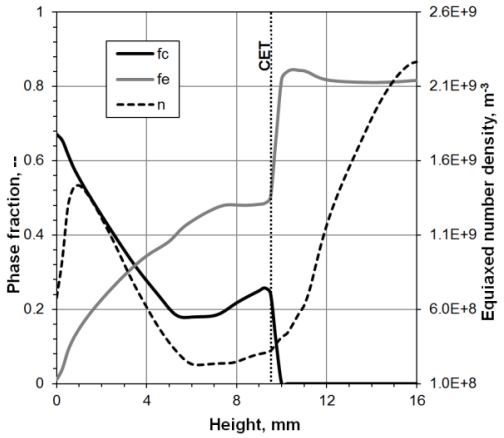

Figure 6. Distribution of f_c, f_e and n versus mould height at 6400 s.

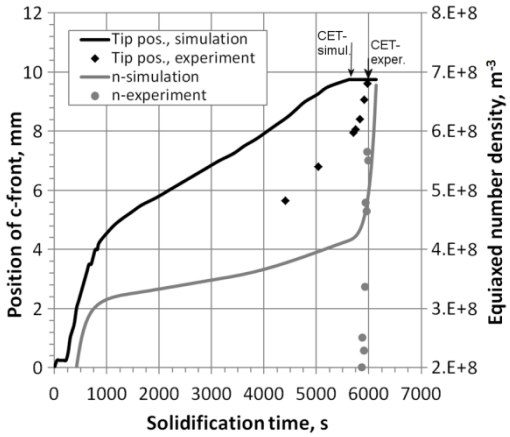

Figure 7. Calculated c-front position and average n *vs* some experimental observations.

The distribution of f_c, f_e and n at 6400 s is plotted versus the mould height as shown in figure 6. Solidification at the bottom starts as columnar. Sudden temperature drop at the bottom after 2 min increases the nucleation rate and correspondingly f_e. The competitive growth between e- and c-phases *is evident below CET (9.5 mm), particularly when the cooling rate increases at 5500 (~8 mm). Thus,* f_c increases but f_e exceeds 0.49 and CET occurs. Ahead of CET f_c= 0 and the nucleation rate increases as the solidification front comes closer to the top.

The development of the position of c-front and the average n in simulation and experiment are plotted during solidification as shown in Figure 7. Initial fast cooling at the bottom causes rapid advancement of c-front which is associated with high nucleation rate. After ~800 s the thermal gradient within the container is stabilized (0). Accordingly, c-front advances linearly and a constant nucleation rate for the equiaxed crystals is obtained. After ~5500 s, the thermal gradient is maintained whereas the cooling rate is increasing. Respectively, the calculated growth rate of c-front is maintained and the nucleation rate of e-phase in the liquid close to c-front increases, leading to blocking of c-front and CET. Calculated and observed CET occur at ~9.5 mm. However, earlier CET is predicted by the model at ~5820 s. A linear growth rate for c-front is observed before 5500 s with relatively faster rate in simulation. After 5500 s the observed c-front advancement rate increases, whereas the calculated

one decreases. The calculated n increases at CET, whereas the observed n increases abruptly. According to experiment, almost no equiaxed crystals form before 5500 s. Formation of equiaxed crystals within the columnar mush is also unobservable.

The calculated undercooling using different laws and the measured one are plotted in Figure 8. The behaviour of ΔT_{exp} and ΔT_{th} are similar, but with ~ 4 K deviation. Measuring ΔT_{exp} did not consider melt constitution [9] and is based on the interpolation of thermocouple readings. ΔT_{con} is applied to equation (1) and (2) and is generally smaller than ΔT_{exp} and ΔT_{th}. Increasing cooling rate after 5500 s increases the concentration of rejected solute in melt. Correspondingly, ΔT_{con} decreases and the growth rate of c-front decreases until CET occurs (Figure 7). The calculated n can also be correlated to the development of ΔT_{con}. Additional experimental and numerical investigations to the estimation of ΔT are still demanding. Practically, observation of nucleation is still ambiguous.

The deviation between observations and the calculations can be attributed to using assumed modelling parameters; k_2 and n_{max}. A parameter study is conducted to estimate the best fit of n_{max} and k_2 to the experiment, two parameter sets are used: (I) k_1= 1.1x10^{-8}, k_2 = 4.55x10^{-8} with variable n_{max}: 4×10^{10} - 8×10^{10} m^{-3}; (II) k_1= 1.1x10^{-8}, n_{max}= 5.0326×10^{10} with variable k_2: 2.66×10^{-8} - 2.8×10^{-8}. The position of CET is plotted versus n_{max} and k_2 for 32 simulation cases as shown in Figure 9. Columnar growth dominates if n_{max}< 5.0×10^{10} m^{-3} or k_2> 2.75×10^{-8} whereas equiaxed solidification dominates if n_{max}> 5.58×10^{10} m^{-3} or k_2< 2.66×10^{-8}. It is obvious that CET is very sensitive to the nucleation parameters of e-phase and to the growth parameters of c-phase. The CET position can be numerically be reproduced by several combinations of the parameters. Here the parameter set (I) with n_{max}= 5.0326×10^{10} m^{-3} and set (II) with k_2 = 2.7368×10^{-8} achieved CET at 9.5 mm but at different times. Further investigations are recommended to determine the proper modelling parameters.

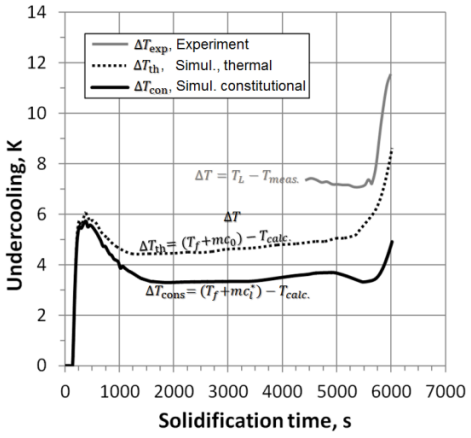

Figure 8. Calculated and measured undercooling at c-front during solidification.

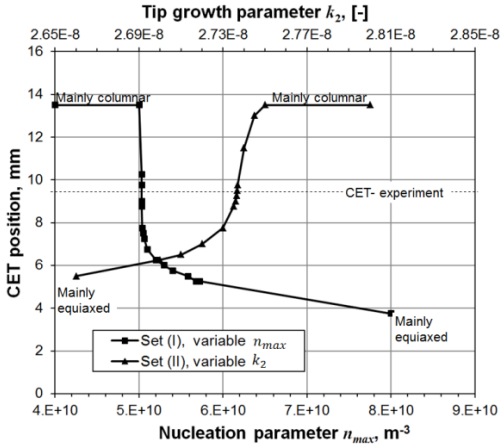

Figure 9. The calculated positions of CET at various n_{max} and k_2 combinations.

6. Conclusion

The 5-phase model might reproduce the solidification structure of µg-experiment including the CET. However, the results are very sensitive to the nucleation parameters of the equiaxed crystals, particularly $\boldsymbol{n_{max}}$, and to the growth parameters of the primary columnar tip, particularly $\boldsymbol{k_2}$. Higher $\boldsymbol{n_{max}}$ promotes the formation of more equiaxed grains and enhances CET. Increasing $\boldsymbol{k_2}$-parameter delays CET. Numerous combinations of $\boldsymbol{n_{max}}$ and $\boldsymbol{k_2}$ can numerically achieve the CET at position which corresponds to experimental one. As future work, the proper set of nucleation and columnar growth parameters has to be experimentally investigated. In addition, the influence of melt flow and crystal sedimentation has to be numerically investigated.

Acknowledgement
This work is financially supported by the FWF Austrian Science Fund (P23155-N24) and the German BMBF (50WM0843).

References

[1] Pötschke M, Gaitzsch U, Roth S, Rellinghaus B and Schultz L 2007 *Magnetism Magnetic Mater.* **316** 383
[2] Wagner A, Shollock B.A and McLean M 2004 *Mat. Sci. Eng. A*, **374** 270
[3] Winegard W and Chalmers B 1954 *Trans. ASM-AIME* **46** 1214
[4] Chalmers B 1963 *J. Austral. Inst. Met.* **8** 255
[5] Jackson K, Hunt J and Uhlmann D Seward III T 1966 *Trans. TMS-AIME* **236** 149
[6] Southin R 1967 *Trans. TMS-AIME* **239** 220
[7] Hunt J 1984 *Mater. Sci. Eng.* **65** 75
[8] Martorano M, Beckermann C and Gandin Ch-A 2003 *Metall. Mater. Trans. A* **34A** 1657
[9] Sturz L and Zimmermann G 2011 *Proc. 20th ESA Symposium on European Rocket and Balloon Programmes and Related Research* vol 700 SP (Hyere: France) p 459
[10] Sturz L and Zimmermann G 2011 J. Physics Conf. Series **327** Article no. 012002
[11] Wu M Ludwig A 2009 *Acta Mater.* **57** 5621
[12] Wu M, Fjeld A and Ludwig A 2010 *Comput. Mater. Sci.* **50** 32
[13] Kurz W and Fisher D.J 1998 *Fundamentals of Solidification* 4th ed (Zurich: Trans Tech)
[14] Lipton J, Glicksman M.E and Kurz W 1984 *Mater. Sci. Eng.* **65** 57
[15] Thevoz Ph and Rappaz M 1989 *Metall. Trans. A* **20A** 311
[16] Rappaz M and Gandin Ch.-A 1993 *Acta Metallurgica et Materialia* **41** 345
[17] Bayrama Ü, Aksöz S and Maraşlı N 2012 *Thermochimica Acta* **531** 12
[18] Witusiewicz V.T, Sturz L, Hecht U and Rex S 2014 *J. Cryst. Growth* **386** 69